Journal of Applied Polymer Science

Synthesis of Amine-Functionalized Block Copolymers for Nanopollutant Removal from Water

Ziyauddin S. Qureshi, Roshan DSouza, Ramakrishna Mallampati, Suresh Valiyaveettil
Department of Chemistry, 3 Science Drive 3, National University of Singapore, Singapore 117 543
Correspondence to: S. Valiyaveettil (E-mail: chmsv@nus.edu.sg)

ABSTRACT: Polyamines are rare in literature owing to increased reactivity, sensitivity to air and moisture, low stability, and processing difficulties. Here, we report the synthesis and characterization of highly processable polyamines and use them for the removal of dissolved metallic nanoparticles from water. Three amphiphilic block polyamines such as poly(*N*-aminoethyl acrylamide-*b*-styrene), poly(*N*-aminopropyl acrylamide-*b*-styrene), and poly(*N*-aminoxylyl acrylamide-*b*-styrene) have been synthesized using atom transfer radical polymerization of ethyl acrylate and styrene followed by aminolysis of the acrylic block. The polymerization and properties of the polymers are studied using different physicochemical techniques. Surface morphology of films prepared from these block copolymers by dissolving in different solvents such as chloroform, tetrahydrofuran and *N,N*-dimethylformamide, and drop-casting polymers on a glass substrate show interesting porous films and spherical nanostructures. In addition, the amine-functionalized block copolymers have been used for the removal of nanoparticles from water and show high extraction efficiency toward silver (Ag) and gold (Au) nanoparticles. All three amine-functionalized block copolymers show higher extraction capacities (Q_e) toward Au NPs (50–109 mg g^{-1}) and Ag NPs (99–117 mg g^{-1}). Our approach allows us to make amine-functionalized block copolymers which are stable in air and can be easily processed in nonpolar solvents. © 2014 Wiley Periodicals, Inc. J. Appl. Polym. Sci. **2014**, *131*, 40943.

KEYWORDS: atom transfer radical polymerization; hydrophilic polymers; kinetics (polym.); self-assembly

Received 23 February 2014; accepted 28 April 2014
DOI: 10.1002/app.40943

INTRODUCTION

Amphiphilic block copolymers are used for several applications such as templates for synthesis of mesoporous materials,[1] in personal care products,[2] oil recovery,[3] and in drug delivery.[4,5] The polymer amphiphiles adopt micellar morphologies in dilute solutions that balance the interfacial energies of the solvated polar block and the hydrophobic block.[2,6] Aqueous dispersions of amphiphilic block copolymers adopt complex structures including spherical, disk or tubular micelles, and vesicles.[2,5–8] Micellar morphologies of polymers depend on several factors such as molecular weight, polydispersity, composition, functionality, solvent conditions, and the method of preparing the dispersion.[5] Water soluble polyacrylamide and its derivatives have played an important role in biomedical applications,[9] waste water treatment,[10] and nontoxic additives in food and paper industries.[11] Polyacrylamides with well-defined structures were prepared using controlled living polymerizations, such as nitroxide mediated radical polymerization,[12] atom transfer radical polymerization (ATRP),[13] the reversible addition-fragmentation chain transfer polymerization,[14] and the cyanoxyl mediated free radical polymerizations.[15,16]

The increased use of metal nanoparticles in various commercial products enhances potential for environmental contamination which may pose serious health concerns in the near future. As nanoparticles showed toxicity in humans and animals,[16–18] it is important to consider methods for their removal from contaminated environment. Nevertheless, a direct separation would be difficult owing to their small size, high reactivity, and large surface area. Recently many groups have reported health concerns caused by metallic nanoparticles to living systems.[19–22] So the removal of such nanoparticles from the environment is a challenge and new methodologies and materials are needed.

Various water purification methods have been developed to remove pollutants, such as chemical coagulation, flocculation, membrane separation, photo-degradation, and ion exchange methods.[23–26] As the research of nanoparticle removal from water is only in the early stages, only a few materials or methods exist for the removal of metal nanomaterial from potable water. Some examples include, studies on the removal of engineered nanoparticles (Ag, TiO_2, and SiO_2) using activated sludge,[27] sorption of silver nanoparticles by activated carbon,[28] and TiO_2 NP's by porous materials.[29] Nevertheless, most of

Additional Supporting Information may be found in the online version of this article.

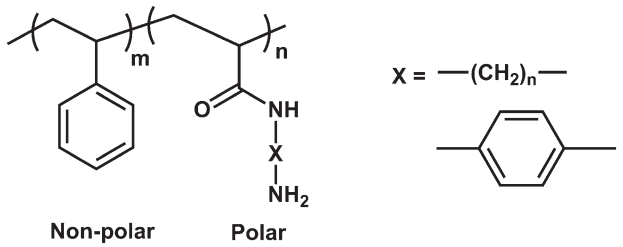

Figure 1. Molecular structure of amine incorporated block copolymers for nanoparticle extraction.

these adsorbents from natural sources exhibited lower extraction efficiencies toward nanoparticles.

In this work, we describe a simple route for the synthesis of a few amine-functionalized poly(*N*-alkyl acrylamide-*b*-styrene)s and study their efficiency toward removal of nanoparticles from water under laboratory conditions (Figure 1). Our approach allows using specially designed polyamines for the removal of nanoparticles. As a model study, the extraction efficiency for the removal of gold and silver nanoparticles from water at moderate pH was evaluated and the observed results are explained using various theoretical models. Incorporating the styrene block is expected to increase the stability of the polymer in ambient conditions.

EXPERIMENTAL

Materials

Ethyl acrylate (EA, 99%), styrene (99%), ethylenediamine (EDA, 98%), 1,3-propylenediamine (PDA, 99%), *p*-xylylenediamine (XDA, 99%), copper(I) bromide (99.9%), ethyl α-bromoisobutyrate (EBIB, 98%), *N*,*N*,*N*′,*N*″,*N*″-pentamethyldiethylenetriamine (PMDETA, 97%), silver nitrate ($AgNO_3$), hydrogen tetrachloroaurate trihydrate ($HAuCl_4$. $3H_2O$), sodium citrate, and sodium borohydride were purchased from Sigma Aldrich. All materials were used without further purification. Chloroform ($CHCl_3$, Fisher Chemical), tetrahydrofuran (THF, BDH Prolabo chemicals) and *N*,*N*-dimethylformamide (DMF, Merck) were used for dissolving block copolymers. Citrate and PVP capped water soluble Au- and Ag-nanoparticles were prepared according to reported procedure[24] and have been summarized in the Supporting Information (SI). Deionised water was used for preparing stock solutions of nanoparticles.

Measurements

Gel permeation chromatography (GPC) for polymers was performed on Waters e2695 alliance system equipped with Waters 2414 refractive index detector using THF as the eluent at a flow rate of 0.3 mL/min at 40°C and polystyrene as standards for calibration. 1H and 13C Nuclear magnetic resonance (NMR)[1] spectra were recorded on Bruker Avance AV300 (300 MHz) NMR instrument using $CDCl_3$ as the solvent. Bruker ALPHA FT-IR spectrophotometer was used for establishing the structure of the polymers. Thermogravimetric analyses (TGA) were conducted using a SDT 2960 TA Instrument. All samples were heated under nitrogen atmosphere from 25 to 800°C using a heating rate of 10°C/min. Differential scanning calorimetry (DSC) measurements were done under nitrogen using a Mettler Toledo DSC1 STAR^e System. Scanning electron microscope (SEM) images for block copolymers were taken with a field emission scanning electron microscopy (FESEM; JEOL JSM-6701F). The samples were mounted on copper stubs with double-sided conducting carbon tape and sputter-coated with 2-nm platinum before examination. The size of the nanoparticles was determined using a transmission electron microscope (TEM, JEOL JEM 2010). The quantitative measurements for nanoparticles were carried out using a UV-Vis spectrophotometer (Shimadzu-1601 PC spectrophotometer).

Synthesis of Macroinitiator

In a typical procedure, a mixture of EA (5 g, 50 mmol), Cu(I)Br (0.07 g, 0.5 mmol), and PMDETA (0.09 g, 0.5 mmol) were taken in a three-neck round bottomed flask, purged with nitrogen for an hour and heated to 80°C.[30] The initiator EBIB (0.097 g, 0.5 mmol) was added to the mixture, heated for 2 h and cooled to room temperature. After diluting with THF, solution was filtered through neutral alumina to remove copper catalyst, the filtrate was concentrated and polymer was precipitated in large excess of *n*-hexane. The solid was redissolved in THF, reprecipitated to yield PEA, and dried under vacuum at 40°C. Yield: 30%, Mn = 3152, polydispersity index (PDI) = 1.18; ^{1}H NMR (300 MHz, $CDCl_3$, δ): 4.1 (—OCH_2—), 2.29 (CH—CO), 1.47 (—CH_2—CH—), 1.25 (CH_3); IR (KBr, cm^{-1}): 2943, 2882 (CH), 1737 (C=O).

Synthesis of Block Copolymers

Styrene (10 g, 96 mmol) was added to a solution of bromo-terminated PEA (4.0 g, 0.5 mmol) in toluene (10 mL).[30] Cu(I)Br (0.072 g, 0.5 mmol) and PMDETA (0.087 g, 0.5 mmol) were added to the mixture. After purging with nitrogen for an hour, the mixture was heated to 110°C and the degree of polymerisation was monitored using GPC analysis at different time-intervals. After 30 h, the reaction was stopped, cooled to room temperature, and diluted with THF. The mixture was filtered through neutral alumina and the solvent was evaporated. Resulting copolymer poly(ethyl acrylate-*b*-styrene) (PEA-*b*-PS) was then precipitated in methanol to yield a white solid which was dried under vacuum for 6 h. Yield: 4.5 g. GPC: Mn = 7257, PDI = 1.10; ^{1}H NMR (300 MHz, $CDCl_3$; δ): 6.43–7.22 (Ar H), 4.13 (—OCH_2—), 2.4(—CH—), 1.93 (—CH—), 1.62 (—CH_2—), 1.29 (—CH_3); IR (KBr, cm^{-1}): 1737 (C=O), 1453, 761, and 700 (phenyl ring).

Aminolysis of Block Copolymers with Different Diamines

A typical aminolysis procedure was followed for the preparation of different amine-functionalized block copolymers. A mixture of PEA-*b*-PS (0.5 g) and diamine (5 g, EDA, PDA, or XDA), taken in a round bottom flask, heated to 120°C and stirred for 48 h to attain homogenous solution. The extent of aminolysis was confirmed by GPC, ^{1}H-NMR, and FT-IR analysis. After completion, the excess diamine was removed either by evaporation (in case of EDA) or by precipitating the polymer in excess of methanol (in case of PDA and XDA). The solid was filtered, washed repeatedly with methanol and dried under high vacuum at 40°C for 16 h.

PAEA-*b*-PS: Yield: 1.23 g; ^{1}H NMR (300 MHz, $CDCl_3$, δ): 6.25–7.2 (Ar H), 5.7 (NH), 1.85 (—CH—), 1.5–1.7 (—CH_2—CH_2—),

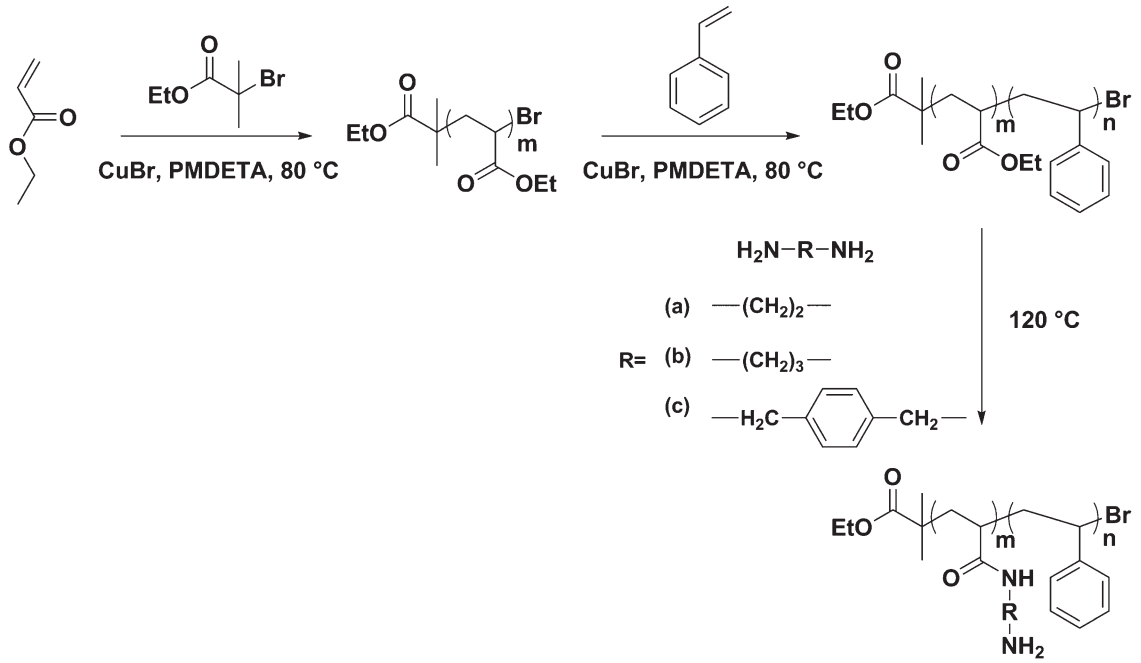

Scheme 1. Preparation of amine-functionalized amphiphilic block copolymers (a) PAEA-*b*-PS, (b) PAPA-*b*-PS, and (c) PAXA-*b*-PS.

1.4 (—CH_2—); IR (KBr, cm^{-1}): 3416, 3370 (NH str), 1725 (C═O), 1650 (—CONH—).

PAPA-*b*-PS: Yield: 1.40 g; ^{1}H NMR (300 MHz, $CDCl_3$, δ): 6.20–7.35 (Ar H), 5.34 (NH), 2.75 (—NH—CH_2—), 1.73 (NH_2—CH_2—), 1.43 (—CH_2—CH_2—CH_2—), 1.25 (—CH_2—); IR (KBr, cm^{-1}): 3441 (NH str), 1737 (C═O), 1650 (—CONH—).

PAXA-*b*-PS: Yield: 1.20 g; ^{1}H NMR (300 MHz, $CDCl_3$, δ): 6.25–7.21 (Ar str), 5.4 (—NH—CH_2—), 3.5 (—OCH_2—), 2.91 (NH_2—CH_2—), 2.02 (—CH—), 1.85 (—CH—), 1.58 (—CH_2—), 0.81 (CH_3—); IR (KBr, cm^{-1}): 3446 (NH str), 1733 (C═O), 1650 (—CONH—).

Extraction of Nanoparticles

To test the extraction efficiency, chloroform solution (400 μL) of amine-functionalized amphiphilic block copolymers (0.001 g/4 mL) was added to a 2 mL centrifuge tube containing aqueous solution of citrate or PVP capped Au- or Ag-nanoparticle (1.5 mL, 2.5 × 10^{-4} *M*) and placed on a mechanical shaker (200 rpm) for 6 h. All extraction experiments were performed at room temperature (26°C) and neutral pH. The residual concentration of nanoparticles was analyzed after predetermined time-interval until the system reached equilibrium. For quantification, nanoparticle solutions were analyzed using UV-Vis spectroscopy periodically to estimate the amount of nanoparticles remained in solution. The nanoparticles extraction capacity Q_e (mg/g) was calculated using the following equation.[31]

$$Q_e = (C_0 - C_e)V/M \quad (1)$$

where C_0 and C_e (mg/L) are initial and equilibrium concentration of nanoparticles, V is the volume of the nanoparticles solution and M is mass of the adsorbent used. In addition, extraction mechanisms of different nanoparticles using amphiphilic block polymers are proposed by studying the extraction kinetics.

RESULTS AND DISCUSSION

Synthesis of amine-functionalized amphiphilic block copolymers is a sequential three step process described in Scheme 1. In the first step, ATRP of EA was done in bulk at 80°C using a molar ratio of [EA] : [CuBr] : [EBIB] as 100 : 1 : 1.

GPC analysis of the resulting poly(ethyl acrylate) showed a number-average molecular weight (Mn) of 3152 with a PDI of 1.18. This PEA macroinitiator was used further for block copolymerization with styrene at 110°C in toluene to obtain the block copolymer, poly(ethyl acrylate-*b*-styrene) (PEA-*b*-PS). GPC analysis of the resulting block copolymer showed a number-average molecular weight (Mn) of 7257 with PDI value of 1.1. In the third step, aminolysis of PEA-*b*-PS was carried out using different diamines (EDA, PDA, or XDA) in a weight ratio of 1 : 10 to get a series of amine-functionalized block copolymers. The number-average molecular weight (Mn) of PAEA-*b*-PS, PAPA-*b*-PS, and PAXA-*b*-PS by GPC imply 30, 32, and 25 repeating units of respective amine-functionalized blocks with 39 units of styrene.

To check the possibility of any degradation of the block to polymer PEA-*b*-PS during reactions with diamines, GPC analyses of the PAEA-*b*-PS, PAPA-*b*-PS and PAXA-*b*-PS polymer samples derived from PEA_{32}-*b*-PS_{38} were performed in THF. The molecular weights of the copolymers after aminolysis are consistent with that of starting polymer (Mn 7257), indicating that the polymers are stable and no degradation took place under

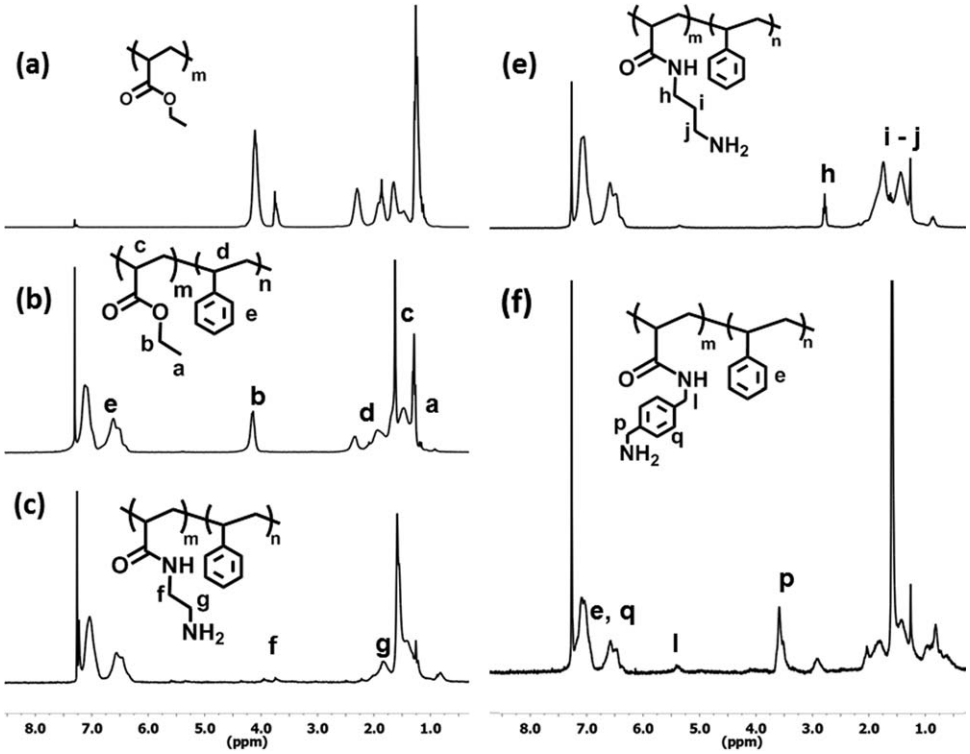

Figure 2. [1]H NMR spectra of macroinitiator PEA (a), block copolymers, PEA-*b*-PS (b), PAEA-*b*-PS (c), PAPA-*b*-PS (d), and PAXA-*b*-PS (e).

aminolysis conditions. GPC analysis showed a single peak with a PDI of 1.14.

[1]H-NMR Study

The structures of amphiphilic block copolymers were established by [1]H-NMR analyses. Figure 2 shows the [1]H-NMR spectra for the step-wise synthesis of amphiphilic block copolymer. The signal due to aliphatic protons appeared in the range from 0.9 to 2.7 ppm, whereas the —CH_2—O— protons of PEA segment showed a broad signal centred at 4.1 ppm [Figure 2(a)]. The signals of aromatic protons of PEA-*b*-PS appeared at 6.3–7.6 ppm [Figure 2(b)]. The integral ratio of the aromatic protons to that of the aliphatic protons is about 1.20, which shows an approximately 38 repeating styrene units in the polystyrene block and 32 repeating units of EA in the PEA block. This implies a molecular weight of 7101 for PAEA-*b*-PS, which is in good agreement with that observed by GPC (Mn = 7257).

Aminolysis of block copolymer PAEA-*b*-PS was carried out using one of the diamines (EDA or PDA or XDA). In case of PAEA-*b*-PS, the signals at 4.1 and 0.9 ppm originating from the ethoxy group of PEA segment disappeared and a new strong signal associated with four protons of methylene unit —NH—CH_2—CH_2—NH_2 groups emerged around 3.7 and 1.58

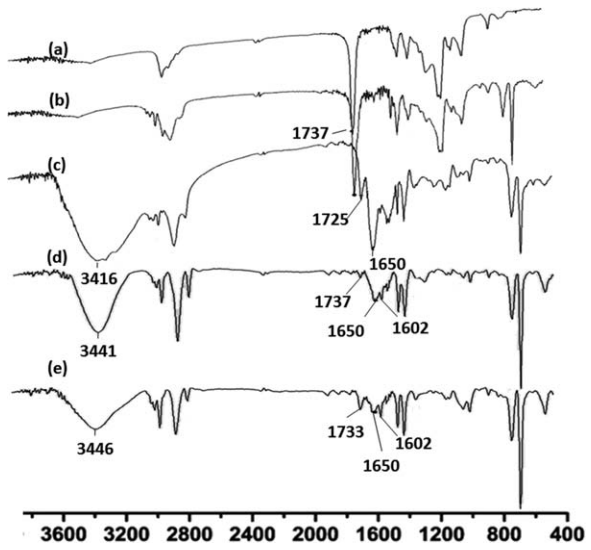

Figure 3. IR spectra for step-wise synthesis of amine-functionalized block copolymers (a) PEA, (b) PEA-*b*-PS, (c) PAEA-*b*-PS, (d) PAPA-*b*-PS, and (e) PAXA-*b*-PS.

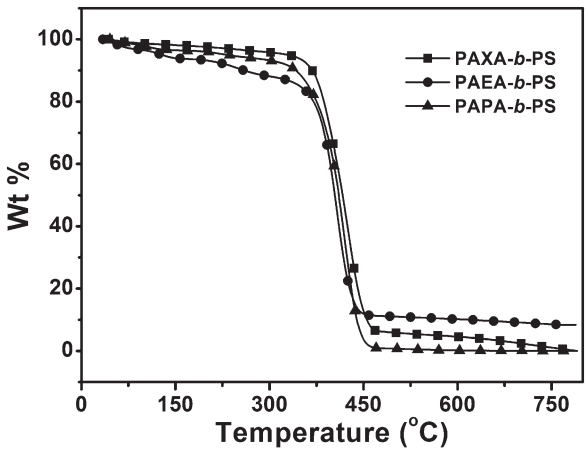

Figure 4. TGA curves of block copolymers in nitrogen atmosphere.

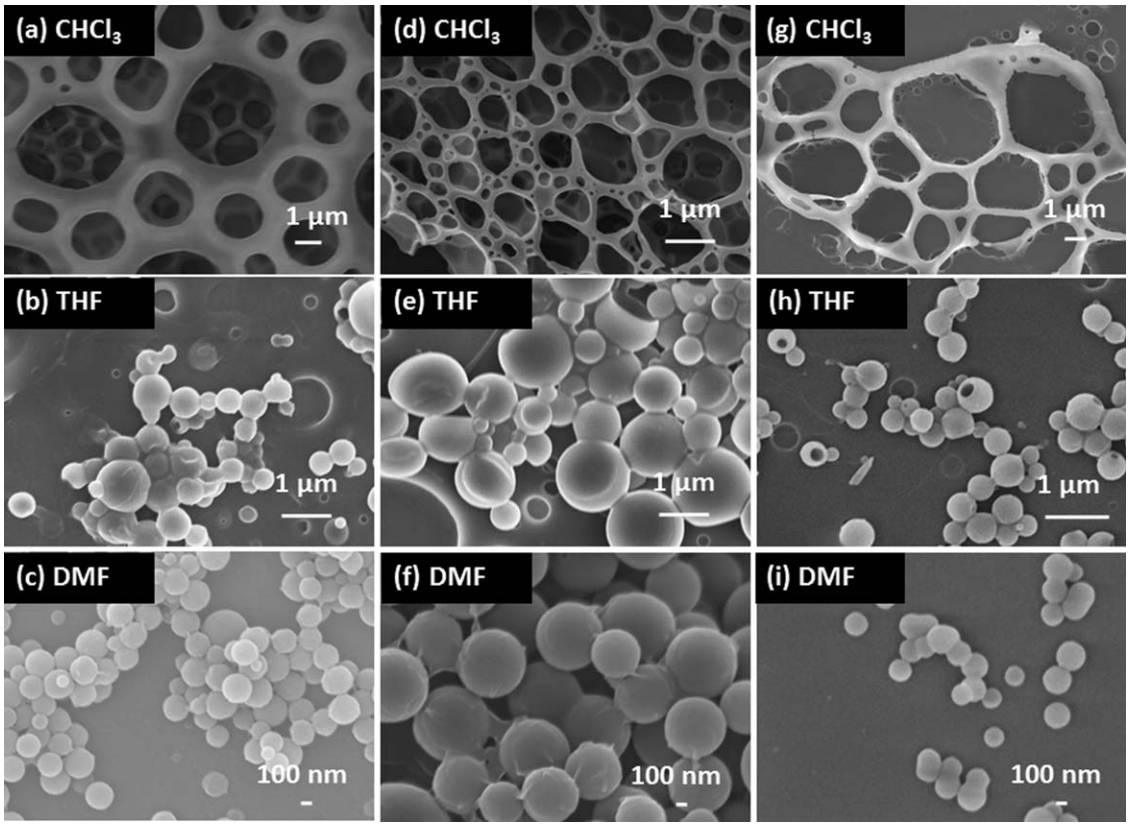

Figure 5. SEM images of the morphology of drop-casted film from PAEA-*b*-PS (a–c), PAPA-*b*-PS (d–f), and PAXA-*b*-PS (g–i) on glass plates from different solvents.

ppm [Figure 2(c)]. A small broad peak at 5.7 ppm can be assigned to the proton of the —NH group. A similar pattern was observed with PAPA-*b*-PS, with multiplets of central methylene protons of propyl appeared at 1.5–2.6 ppm and NH peak was seen at 5.3 ppm [Figure 2(d)]. These results imply aminolysis of PEA segment of the block copolymer with both EDA and PDA. The ^{1}H-NMR spectra of PAXA-*b*-PS shows peaks at 2.9 and 5.4 ppm corresponds to —CH_2NH_2 and —$NHCH_2$, respectively, while —CH_2—O— protons of PEA segment appeared at 3.58 ppm [Figure 2(e)] indicating only a partial aminolysis. There have been earlier reports which describe such aminolysis reactions of esters with different amines giving the corresponding amide compounds.[30,32]

FT-IR Analysis

FT-IR spectra of the polymers obtained in each step of chemical transformations are shown in Figure 3. In Figure 3(a), the characteristic carbonyl stretching of the starting PEA appears at 1737 cm^{-1}. The other typical peaks observed at 1258 and 1161 cm^{-1} are associated with stretching vibrations of (O═C)—O and O—CH_2 bonds, respectively. Similar peaks were obtained after copolymerization with styrene block [Figure 3(b)] and the new peaks of the polystyrene block emerged in the spectrum. The peaks observed at 1590 and 1600 cm^{-1} are assigned to stretching vibrations of aromatic C—C bond. Aminolysis in the third step results in complete disappearance of carbonyl peak of PEA at 1737 cm^{-1} and appearance of a new peak associated with the amide carbonyl at 1650 cm^{-1} [Figure 3(c)], which indicates quantitative aminolysis of the ester function with diamines. The broad band around 3300–3650 cm^{-1} range can be ascribed to stretching vibration of N—H bond. IR spectra of PAEA-*b*-PS and PAPA-*b*-PS reconfirms complete aminolysis of polyether block [Figure 3(c,d)], while IR spectra of PAXA-*b*-PS shows notable peaks for both the carbonyl ester and amide at 1733 and 1650 cm^{-1}, respectively, suggesting only a partial aminolysis [Figure 3(e)].

Thermal Properties (TGA and DSC Analyses)

To understand the thermal stability of the amphiphilic block polymers, the thermogravimetric analysis (TGA) and DSC were performed under nitrogen atmosphere. TGA curves of all copolymers are shown in Figure 4, which suggest comparable thermal stabilities for all three copolymers. In case of PAEA-*b*-PS, an initial small loss (3% weight at 100°C) can be attributed to the loss of trace amounts of water and residual solvents in the sample. The polymers are stable up to 300°C and start to degrade at 375–400°C until 450°C leaving a little or no carbonaceous residues.

The glass transition temperature (T_g) observed in the DSC analyses show an increasing stiffness in the block copolymers with the introduction of strong intermolecular interactions through H-bonding by amide groups, when compared to the ester segment of PAEA-*b*-PS copolymer. The T_g of PEA-*b*-PS is 78°C and those of the block copolymers PAEA-*b*-PS, PAPA-*b*-PS, and

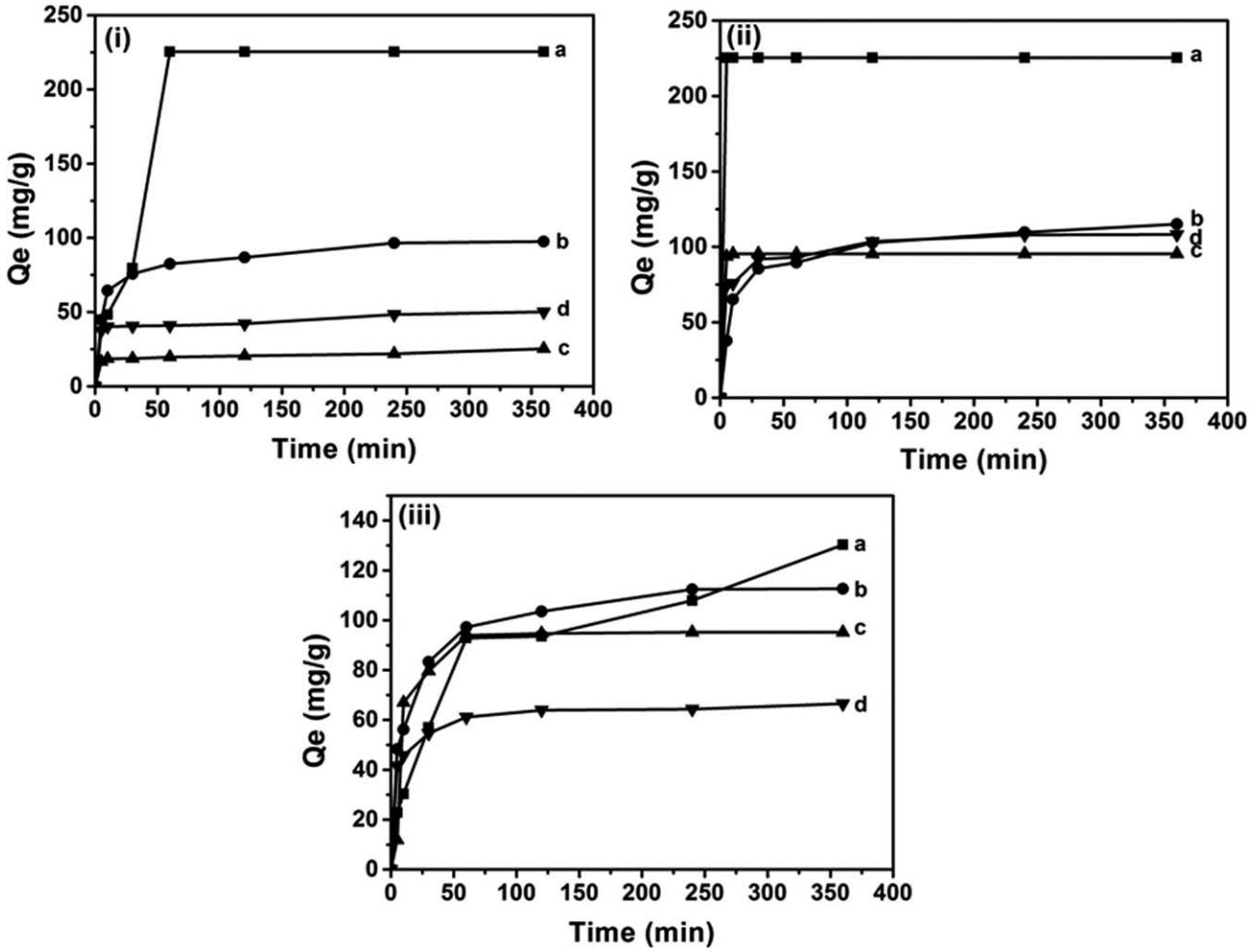

Figure 6. Variation of extraction efficiency with change in time for (i) PAEA-*b*-PS, (ii) PAPA-*b*-PS, and (iii) PAXA-*b*-PS copolymers with (a) Ag(Ct), (b) Ag(PVP), (c) Au(Ct), and (d) Au(PVP) nanoparticles.

PAXA-*b*-PS are increased to 86, 93, and 103°C, respectively, with increased alkyl chain and aromatic units. All DSC traces are shown in SI Figure SI-3.

Self-Assembly of Polymers

Block copolymers self-assemble into diverse morphologies depending on the relative fractions of the hydrophobic and hydrophilic blocks.[7,8] Different polymer-solvent interactions and properties of solvents are known to control the structure of the micelles and their ordered packing.[33,34]

In the present study, thin films of the block copolymers (PAEA-*b*-PS, PAPA-*b*-PS, and PAXA-*b*-PS) were prepared on glass slides by drop-casting solutions of polymers (1 mg mL^{-1}) in different solvents ($CHCl_3$, THF, and DMF) at room temperature. FESEM was used to establish the self-assembly of block copolymers (Figure 5). When the block copolymers dissolved in $CHCl_3$ were drop-casted on a glass substrate, ordered porous films were formed for all the three copolymers in less than 60 s with the solvent evaporation, as seen by FESEM studies. However, the shape regularity of PAPA-*b*-PS and PAXA-*b*-PS films was low in comparison to that formed by PAEA-*b*-PS.

The difference in the formation of breath figures can be explained owing to the presence of amphiphilic character for all block copolymer backbone, which may help to form certain structures under ambient conditions and high humidity.[35] We suggest that porous network structure was formed owing to the evaporation of low-boiling hydrophobic solvents under high humidity, followed by water of condensation and evaporation, similar to breath figure formation.[32,33,36–38] In contrast to this, the polymer solutions in polar, high-boiling solvents such as THF and DMF formed spherical polymer nanospheres (100–650 nm) on solvent evaporation. Here, the spherical micelles formation is preferred owing to the high polarity of the solvent. The observed morphology is also dependent on the relative composition of solvent and initial polymer concentration. At a low polymer concentration (1 mg mL^{-1}), spherical nanoparticles were formed, while highly aggregated spherical structures were observed when the polymer concentrations were increased further.

Extraction of Metal Nanoparticles from Aqueous Solution

Citrate and PVP capped Au- and Ag-nanoparticles were synthesized in our lab and are fully characterized. The size of the synthesized spherical Au NPs (15–20 nm) and Ag NPs (20–40 nm)

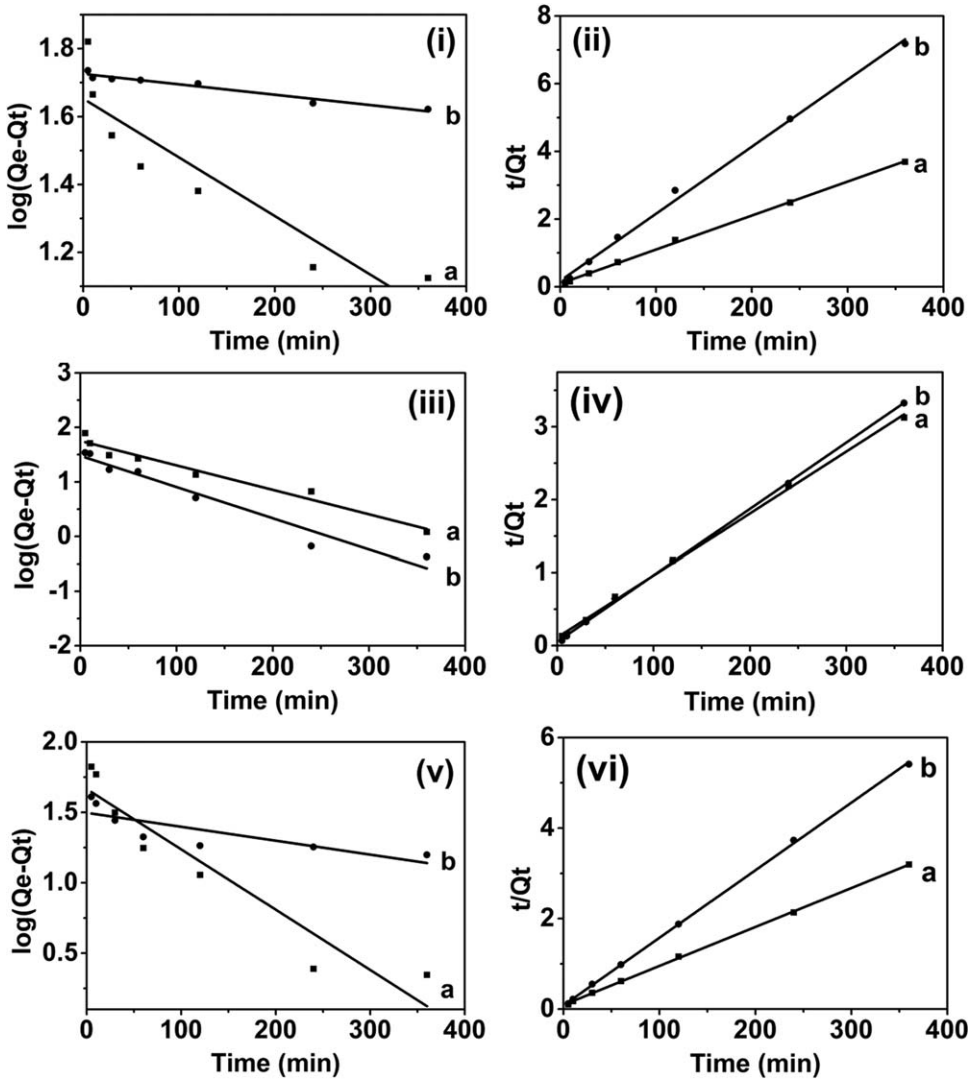

Figure 7. Pseudo-first-order (i, iii, v) and pseudo-second-order (ii, iv, vi) kinetics for copolymers PAEA-*b*-PS (i, ii), PAPA-*b*-PS (iii, iv), and PAXA-*b*-PS (v, vi) for extraction of nanoparticles (a) Ag(PVP) and (b) Au(PVP).

were characterized using TEM. UV-Vis spectra of Au and Ag NPs showed absorbance maxima at 518 nm and at 420 nm, respectively (ESI).

The extraction capacities of all three block copolymers (PAEA-*b*-PS, PAPA-*b*-PS, and PAXA-*b*-PS) with respect to the nanoparticles and extraction time were determined. Extraction experiments were done using initial nanoparticle concentrations of (1.5 mL, 2.5×10^{-4} *M*) at neutral pH and extraction kinetic data were deduced from the experimental data. The amount of nanoparticles extracted using block copolymers increased with time and a dynamic equilibrium was reached rapidly (20 min),

Table I. Pseudo-First-Order and Pseudo-Second-Order Constants and Correlation Coefficients for Extraction of Nanoparticles with Block Copolymers

			Pseudo-first-order kinetic model			Pseudo-second-order kinetic model		
Polymers	NP's	Q_e (exp; mg/g)	Q_e (mg/g)	k_1 (min^{-1})	R^2	Q_e (mg/g)	k_2 (g/mg min)	R^2
PAEA-*b*-PS	Ag(PVP)	97.4888	44.9666	0.0039	0.8027	99.6016	0.0010	0.9988
	Au(PVP)	50.1300	53.1361	0.0007	0.9443	50.4541	0.0022	0.9958
PAPA-*b*-PS	Ag(PVP)	115.1780	56.4040	0.0103	0.9581	117.7860	0.0006	0.9985
	Au(PVP)	108.2180	30.0725	0.0132	0.9498	109.8900	0.0015	0.9995
PAXA-*b*-PS	Ag(PVP)	112.6690	46.3458	0.0099	0.8900	116.1440	0.0008	0.9996
	Au(PVP)	66.5100	31.3545	0.0023	0.6192	66.9344	0.0027	0.9996

especially in the case of citrate capped Ag NPs, owing to strong interaction of the polymers and nanoparticles (ESI). The observed extraction efficiencies could be explained based on a combination of both electrostatic and strong interaction between amines and Ag NP surface.[39] The extraction efficiencies of PAEA-*b*-PS and PAPA-*b*-PS were considerably higher than those of PAXA-*b*-PS for all four nanoparticles (Figure 6). This phenomenon could be attributed to low degree of aminolysis of PAXA-*b*-PS as compared to the PAEA-*b*-PS and PAPA-*b*-PS.

Extraction Kinetics

Different kinetic models have been used to explain the extraction of nanoparticles using our polymers.[40–42] To investigate the extraction kinetics for the four nanoparticles, the pseudo-first-order [eq. (2)] and second-order [eq. (3)] equations were used to analyse the experimental data from the three polymers, PAEA-*b*-PS, PAPA-*b*-PS, and PAXA-*b*-PS using standard nanoparticle concentration within 6 h of extraction time (Figure 7).

$$\text{Pseudo-first-order:}\quad \text{Log}\ (Q_e - Q_t) = \text{Log}\, Q_e - k_1 t/2.303 \qquad (2)$$

$$\text{Pseudo-second-order:}\quad t/Q_t = 1/k_2 Q_e^{\,2} + t/Q_e \qquad (3)$$

where, Q_e and Q_t indicate the amount of dye adsorbed (mg g^{-1}) at equilibrium and at time t, respectively whereas k_1 (min^{-1}) and k_2 (g mg^{-1}min) were the corresponding extraction rate constants.

Extraction studies were carried out using polymer solutions at two concentrations (0.5 and 0.25 mg/mL) in $CHCl_3$. It was found that use of high polymer concentration (0.5 mg/mL) led to high extraction efficiency within a few minutes. Hence, further extractions were carried out using 0.25 mg/mL polymer solution to study the extraction kinetics. In case of Ag(Ct) and Au(Ct) NPs, the equilibrium was reached within 10 min and deduction of different kinetic parameters for such fast extraction process is not manageable.

The results of the rate constants for the first-order and second-order extraction kinetics for all four nanoparticles with different block copolymers are summarized in Table I. It could be seen that the correlation coefficients (R^2) from second-order extraction kinetics fits well with the experimental data compared to the pseudo-first-order model. Also, the calculated Q_e values from the second-order model were in accordance with the experimental data. These results indicated that the extraction follows the second-order extraction kinetics for all three block copolymers.

CONCLUSIONS

In conclusion, synthesis of polyamines was achieved from PEA-*b*-PS via aminolysis of the PEA block with different diamines (e.g., EDA, PDA, and XDA). This synthetic strategy is versatile and can be adapted to different amines to prepare interesting processable and stable polyamines. All prepared amphiphilic block copolymers exhibited good solubility in common organic solvents and thermal stability. Also a simple, yet versatile route to fabricate ordered porous films or spherical particles of these block polyamines via simple drop-casting method is established. A porous morphology was obtained from hydrophobic $CHCl_3$ and spherical morphologies from polar solvents like THF and DMF. Furthermore, application of such polyamines for the extraction of nanoparticles from aqueous medium at moderate pH was demonstrated. The block copolymers were found to be highly efficient in extracting emerging pollutants such as Ag- and Au-nanoparticles from aqueous environment. All block copolymers showed a high value of Qe for both citrate and PVP capped Ag- and Au-nanoparticles. Such macromolecules may be used for purification of contaminated water.

ACKNOWLEDGMENTS

The authors gratefully acknowledge the financial support from the Environment and Water Industry Programme Office (EWI) under the National Research Foundation of Singapore (PUBPP 21100/36/2, NUS WBS R-706-002-013-290, R-143-000-458-750, R-143-000-458-731). They also thank the Department of Chemistry, National University of Singapore and NUS Environmental Research Institute (NERI) for all technical support.

REFERENCES

1. Finnefrock, A. C.; Ulrich, R.; Toombes, G. E. S.; Gruner, S. M.; Wiesner, U. *J. Am. Chem. Soc.* **2003**, *125*, 13084.
2. Discher, D. E.; Eisenberg, A. *Science* **2002**, *297*, 967.
3. Morgan, S. E.; McCormick, C. L. *Prog. Polym. Sci.* **1990**, *15*, 103.
4. Geng, Y.; Discher, D. E. *ACS Symp. Ser.* **2006**, *939*, 168.
5. Hayward, R. C.; Pochan, D. *J. Macromolecules* **2010**, *43*, 3577.
6. Gohy, J.-F.; *Adv. Polym. Sci.* **2005**, *190*, 65.
7. Jain, S.; Bates, F. S. *Science* **2003**, *300*, 460.
8. Jain, S.; Bates, F. S. *Macromolecules* **2004**, *37*, 1511.
9. Liu, P.; Zhang, S.; Yang, N.; Xiong, C. *Pet. Explor. Dev.* **2012**, *39*, 619.
10. Zhu, J.; Zheng, H.; Jiang, Z.; Zhang, Z.; Liu, L.; Sun, Y.; Tshukudu, T. *Desalin. Water Treat.* **2013**, *51*, 2791.
11. Yuan, Z.; Hu, H. *J. Appl. Polym. Sci.* **2012**, *126*, E459.
12. Hawker, C. J.; Bosman, A. W.; Harth, E. *Chem. Rev.* **2001**, *101*, 3661.
13. Matyjaszewski, K.; Xia, J. H. *Chem. Rev.* **2001**, *101*, 2921.
14. Kamigaito, M.; Ando, T.; Sawamoto, M. *Chem. Rev.* **2001**, *101*, 3689.
15. Moad, G.; Rizzardo, E.; Thang, S. H. *Aust. J. Chem.* **2005**, *58*, 379.
16. Grande, D.; Baskaran, S.; Baskaran, C.; Gnanou, Y.; Chaikof, E. L. *Macromolecules* **2000**, *33*, 1123.
17. Teow, Y.; Asharani, P. V.; Hande, M. P.; Valiyaveettil, S. *Chem. Commun.* **2011**, *47*, 7025.
18. Khlebtsov, N.; Dykman, L. *Chem. Soc. Rev.* **2011**, *40*, 1647.
19. Teodoro, J. S.; Simões, A. M.; Duarte, F. V.; Rolo, A. P.; Murdoch, R. C.; Hussain, S. M.; Palmeira, C. M. *Toxicol. In Vitro* **2011**, *25*, 664.
20. Frohlich, E.; Samberger, C.; Kueznik, T.; Absenger, M.; Roblegg, E.; Zimmer, A.; Pieber, T. R. *J. Toxicol. Sci.* **2009**, *34*, 363.

21. Asharani, P. V.; Yi, L. W.; Gong, Z. Y.; Valiyaveettil, S. *Nanotoxicology* **2011**, *5*, 43.
22. Asharani, P. V.; Mun, G. L. K.; Hande, M. P.; Valiyaveettil, S. *ACS Nano* **2009**, *3*, 279.
23. Asharani, P. V.; Sethu, S.; Vadukumpully, S.; Zhong, S. P.; Lim, C. T.; Hande, M. P.; Valiyaveettil, S. *Adv. Funct. Mater.* **2010**, *20*, 1233.
24. Mahanta, N.; Leong, W. Y.; Valiyaveettil, S. *J. Mater. Chem.* **2012**, *22*, 1985.
25. Mallampati, R.; Valiyaveettil, S. *J. Nanosci. Nanotechnol.* **2012**, *12*, 618.
26. Fernandes, A.; Morão, A.; Magrinho, M.; Lopes, A.; Gonçalves, I. *Dyes Pigm.* **2004**, *61*, 287.
27. Park, H.-J.; Kim, H. Y.; Cha, S.; Ahn, C. H.; Roh, J.; Park, S.; Kim, S.; Choi, K.; Yi, J.; Kim, Y.; Yoon, J. *Chemosphere* **2013**, *92*, 524.
28. Gicheva, G.; Yordanov, G. *Colloids Surf. A* **2013**, *431*, 51.
29. Rottman, J.; Platt, L. C.; Sierra-Alvarez, R.; Shadman, F. *Chem. Eng. J.* **2013**, *217*, 212.
30. Deniz, G.; Omer, B. K.; Niyazi, B. J. *J. Appl. Polym. Sci.* **2013**, *127*, 2684.
31. Ramakrishna, M.; Valiyaveettil, S. *RSC Adv.* **2012**, *2*, 9914.
32. Bekheit, M. M.; Nawar, N.; Addison, A. W.; Abdel-Latif, D. A.; Moniera, M. *Int. J. Biol. Macromol.* **2011**, *48*, 558.
33. Lodge, T. P.; Pudil, B.; Hanley, K. *J. Macromolecules* **2002**, *35*, 4707.
34. Park, M. J.; Char, K.; Bang, J.; Lodge, T. P. *Macromolecules* **2005**, *38*, 2449.
35. Nurmawati, M. H.; Renu, R.; Ajikumar, P. K.; Sindhu, S.; Cheong, F. C.; Sow, C. H.; Valiyaveettil, S. *Adv. Funct. Mater.* **2006**, *16*, 2340.
36. Guo, Z. S.; Pei, J.; Zhou, Z. L.; Zhao, L.; Gibson, G.; Lam, S.; Brug, J. *Polymer* **2009**, *50*, 4794.
37. Deepak, V. D.; Asha, S. K. *J. Phys. Chem. B* **2006**, *110*, 21450.
38. Dianjun, Y.; Bindu, T.; Pudupadi, R. S. *Macromolecules* **2006**, *39*, 7786.
39. Nath, S.; Ghosh, S. K.; Kundu, S.; Praharaj, S.; Panigrahi, S.; Pal, T.; *J. Nanopart. Res.* **2006**, *8*, 111.
40. Verma, V. K.; Mishra, A. K. *Global Nest. J.* **2010**, *12*, 190.
41. Duran, C.; Ozdes, D.; Gundogdu, A.; Senturk, H. B.; *J. Chem. Eng. Data* **2011**, *56*, 2136.
42. Bhattacharyya, K. G.; Gupta, S. S. *Desalination* **2011**, *272*, 66.